

Electronic Supplementary Information

for

Versatile Plasmonic Effects at the Interface of Inverted Perovskite
Solar Cells

Ahmed Esmail Shalan^a, Tomoya Oshikiri^a, Hiroki Sawayanagi^a, Keisuke Nakamura^a, Kosei Ueno^a, Quan Sun^a, Hui-Ping Wu^b, Eric Wei-Guang Diau^{b} and Hiroaki Misawa^{a,b*}*

[a] Mr. Ahmed Esmail Shalan, Mr. Hiroki Sawayanagi, Mr. Keisuke Nakamura,
Prof. Dr. K. Ueno, Prof. Dr. T. Oshikiri, Prof. Dr. H. Misawa

Research Institute for Electronic Science, Hokkaido University, N21, W10, Kita-ku,
001-0021, Sapporo (Japan)

E-mail: misawa@es.hokudai.ac.jp, diau@mail.nctu.edu.tw

[b] Dr. Hui-Ping Wu, Prof. Dr. Eric Wei-Guang Diau, Prof. Dr. H. Misawa

Department of Applied Chemistry & Institute of Molecular Science, National
Chiao Tung University, 1001 Ta Hsueh R., Hsinchu 30010 (Taiwan), ROC

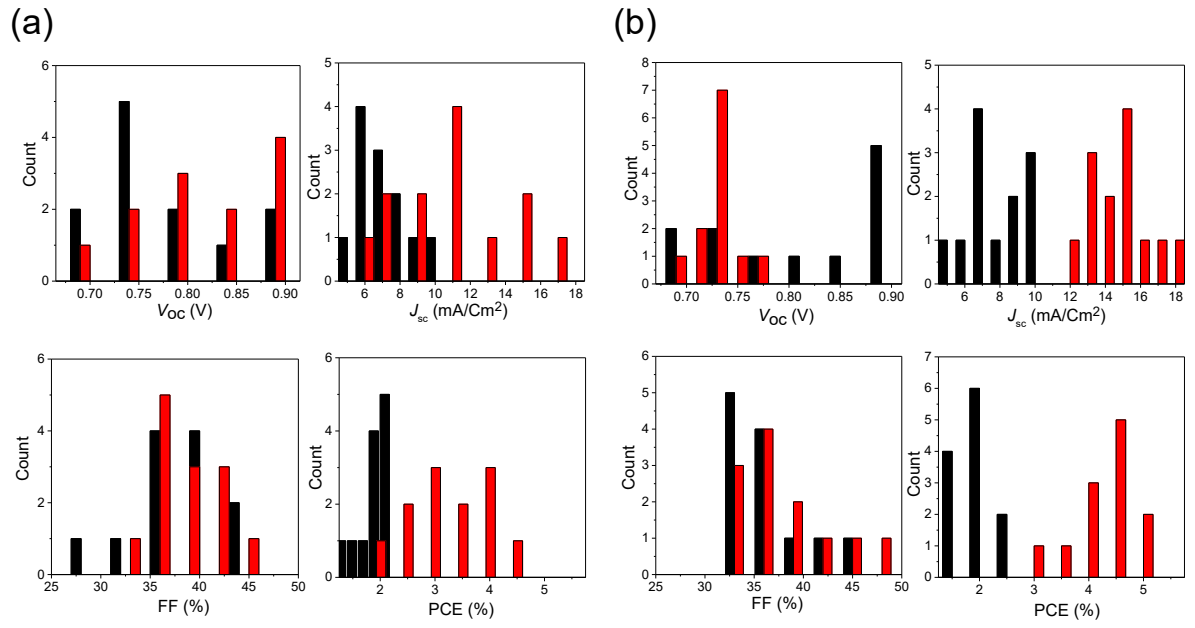


Figure S1. Device reproducibility. Histograms of devices performance parameters V_{oc} , J_{sc} , FF and PCEs for 24 perovskite solar cells with 5-nm-thick (a) and 10-nm-thick (b) NiO. Black and red bars indicate devices without and with Au NIs, respectively.

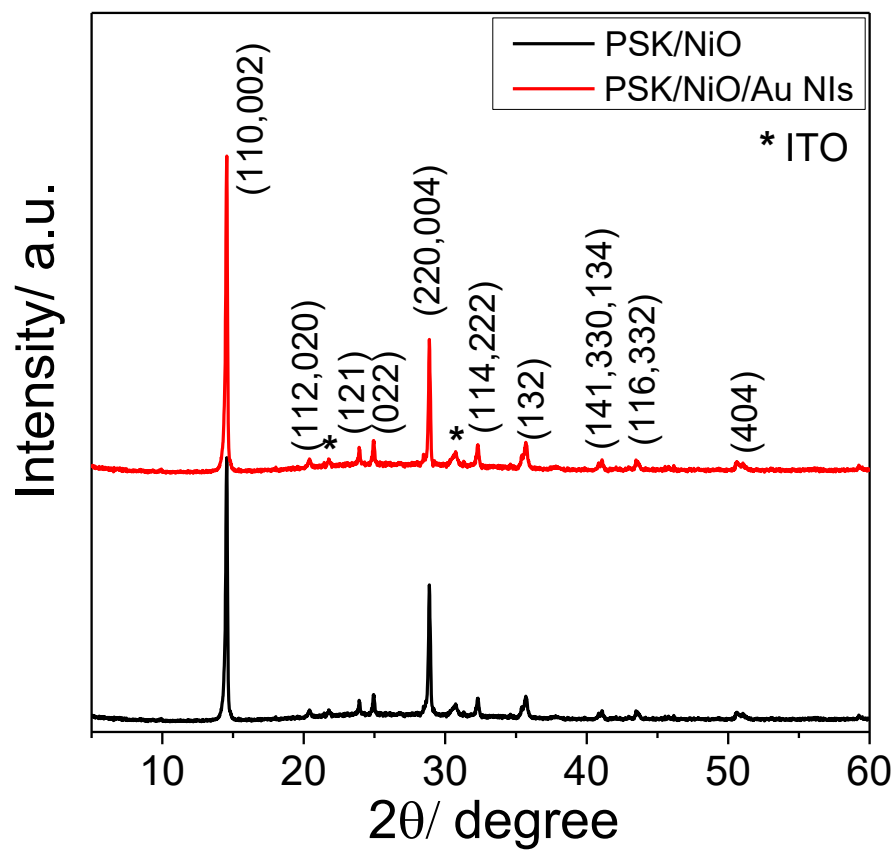


Figure S2. XRD patterns of the PSK film onto the NiO film with (red) and without (black) Au NIs.

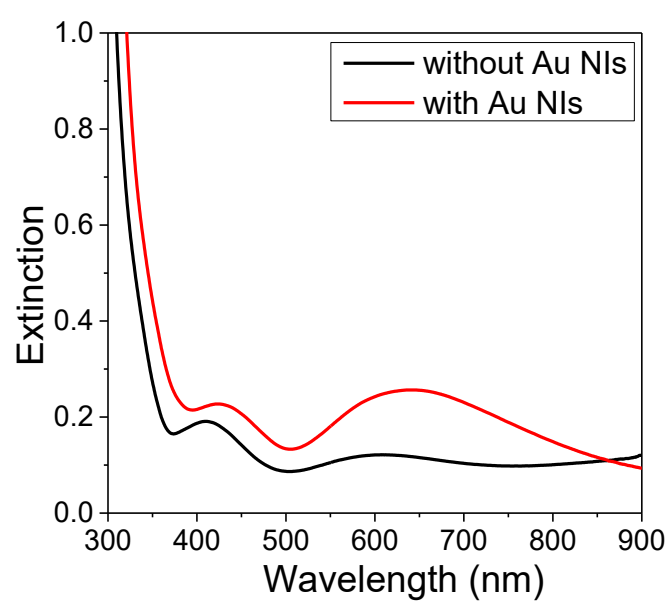


Figure S3. Extinction spectra of the sample with 10-nm-thick NiO in the presence and the absence of Au NIs. The extinction spectra are obtained in the absence of perovskite layer.

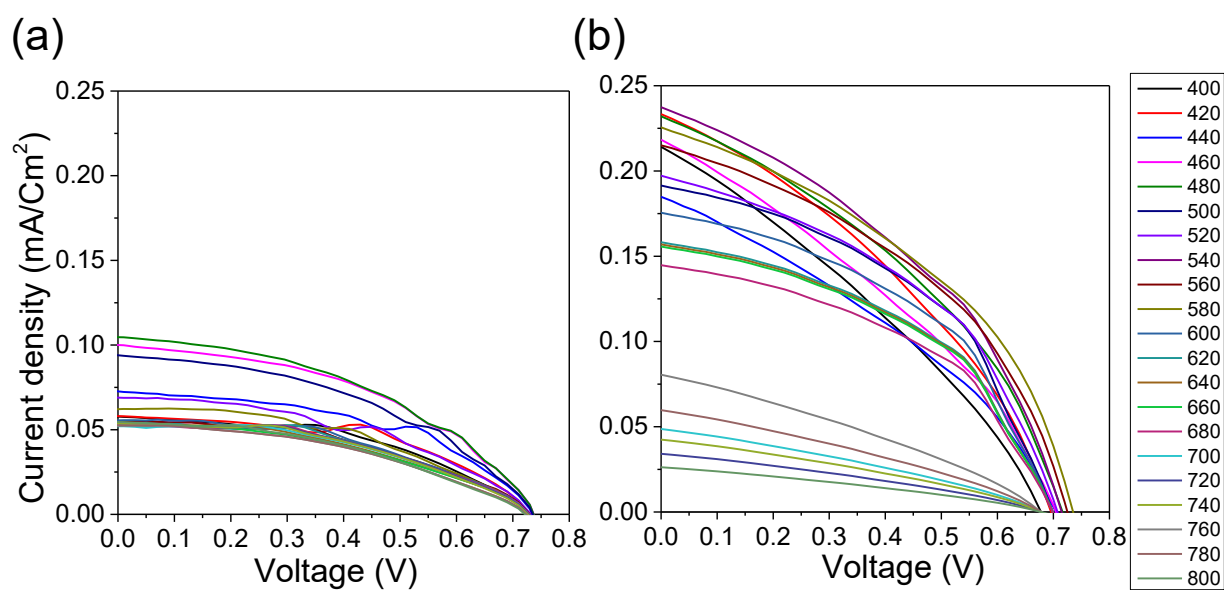


Figure S4. J - V characteristics of ITO/NiO/PSK/PCBM/Ag in the absence (a) and presence (b) of Au NIs at each wavelength (400-800 nm) in the presence of band pass filter for the incident light. The thickness of the NiO was 10 nm.

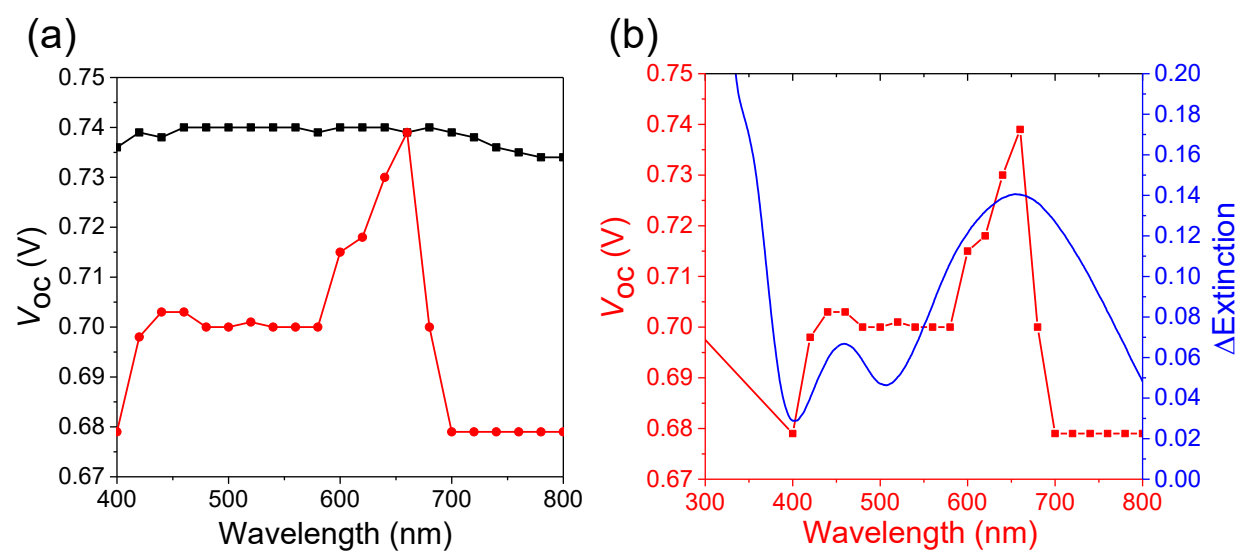


Figure S5. (a) The difference of V_{oc} values at each wavelength (400-800 nm) in the absence (black) and the presence (red) of Au NIs. (b) A relation between the V_{oc} values and the LSPR represented by $\Delta\text{extinction}$ spectrum. The thickness of the NiO was 10 nm.

Statistical analysis of the Au-NPs particle size distribution

A scanning electron microscope image of the Au-NPs on NiO-PLD was used for statistical analysis of the Au-NPs particle size distribution based on the usage of free software ImageJ (<http://rsb.info.nih.gov/ij/>). Subsequently, top-view SEM micrographs of the Au-NIs-loaded NiO thin films with thicknesses of 10 and 5 nm are shown in Figure S6a and 6b, respectively. The NiO surface morphology indicated significant surface roughening. The Au-NIs loaded on NiO 10 nm thin film exhibited particle size distributions smaller than NiO 5 nm and both seems to be nearly round shapes when viewed from the top, and the statistical analysis of the particles for NiO 10 and 5 nm revealed an average size distribution of 40.1 and 53.0 nm in diameter with a standard deviation of approximately 28.8 and 35.8 nm, respectively as calculated from (Figure S6c and S6d).

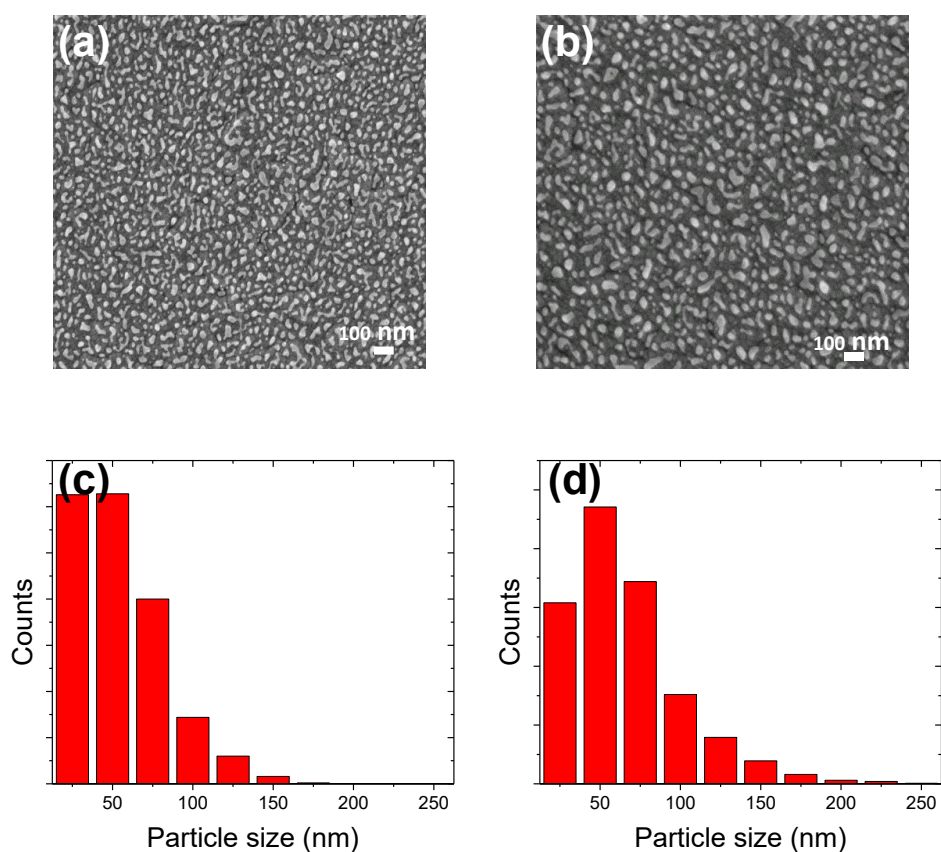


Figure S6. The SEM images of Au NIs on 10-nm-thick NiO film (a) and 5-nm-thick NiO film (b), respectively. (c), (d) Histograms of the particle diameters of (a) and (b) samples, respectively.

Characterizations of perovskite solar cells

The structure and morphology of the $\text{CH}_3\text{NH}_3\text{PbI}_3$ films were investigated by X-ray diffraction (XRD), X-ray photoelectron Spectroscopy (XPS) and cross-sectional scanning electron microscopy (SEM) measurements (Fig. S7). To investigate the XRD data, PSK were fabricated on ITO. As shown in Fig. S7a, the XRD peak positions for ITO and $\text{CH}_3\text{NH}_3\text{PbI}_3$ films on ITO substrate are studied. The diffraction peaks at 14.10° , 20.01° , 23.48° , 24.50° , 28.45° , 31.89° , 34.98° , 40.68° , 42.59° , 43.20° , and 50.22° correspond to planes (110, 002), (112, 020), (121), (022), (220,004), (114, 222), (132), (141, 330, 134), (116, 332) and (404) of the $\text{CH}_3\text{NH}_3\text{PbI}_3$ tetragonal phase, indicating the fully formed perovskite structure from the $\text{CH}_3\text{NH}_3\text{I}$ and the PbI_2 .^{S1, S2} No impurity peaks are detected, indicating that the grown perovskite structures were of high purity and good crystallinity. The asterisks in the chart refer to ITO peaks. Furthermore, Fig. S7b show the Pd 4f and I 3d regions of the XPS spectra of perovskite films on ITO and NiO. The binding energies with Pb 4f and with I 3d core levels is in good agreement with Lindblad's results.^{S3} It also shows a single of I $3d_{5/2}$ core level at a binding energy of approximately 619.5 eV for both NiO/ $\text{CH}_3\text{NH}_3\text{PbI}_3$ and ITO/ $\text{CH}_3\text{NH}_3\text{PbI}_3$ samples with a spin-orbit split of 11.5 eV to the I $3d_{3/2}$ level for all samples. The binding energy distance between the Pb 4f and the I 3d core planes is equal in all samples.

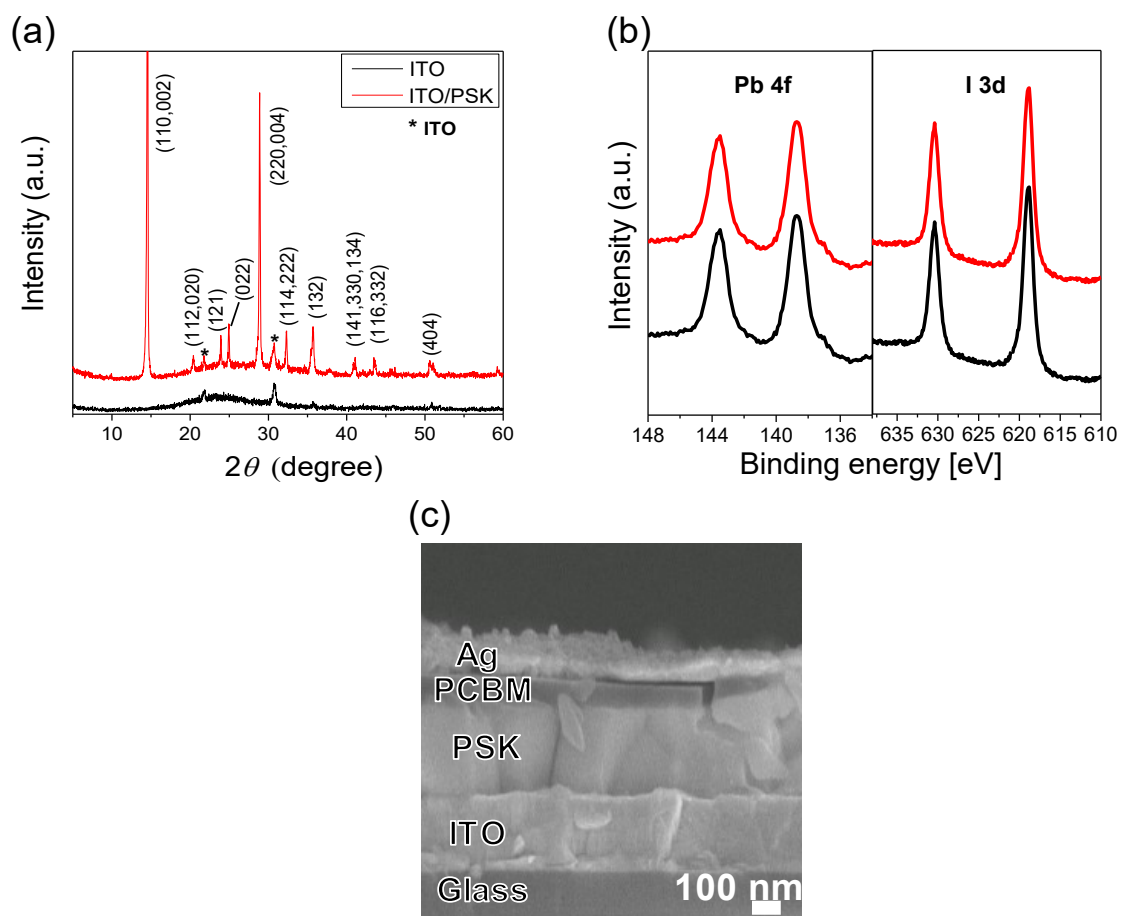


Figure S7. Fabrication information on perovskite solar cells. (a) XRD patterns of the $\text{CH}_3\text{NH}_3\text{PbI}_3$ film obtained via spin coating process onto the ITO surface. All of the peaks are perovskite the X-ray diffraction expect for small ITO diffraction peaks labeled. (b) XPS spectra of Pb 4f and I 3d as a component of the PSKe deposited on the ITO (black line) and the NiO (red line). (c) The cross-sectional SEM image of ITO/NiO/PSK/PCBM/Ag. The NiO film between the ITO and the PSK is not observed because the film is too thin.

References and Notes

- (S1) K. Liang, D. B. Mitzi and M. T. Prikas, *Chem. Mater.*, 1998, 10, 403.
- (S2) N. J. Jeon, J. H. Noh, Y. C. Kim, W. S. Yang, S. Ryu and S. I. Seok, *Nat. Mater.*, 2014, 13, 897.
- (S3) R. Lindblad, D. Bi, B. Park, J. Oscarsson, M. Gorgoi, H. Siegbahn, M. Odelius, E. M. J. Johansson and H. Rensmo, *J. Phys. Chem. Lett.*, 2014, 5, 648–653.